AGU PUBLICATIONS

Geophysical Research Letters

RESEARCH LETTER
10.1002/2016GL069626

Special Section:
First results from NASA's Magnetospheric Multiscale (MMS) Mission

Comparison of Magnetospheric Multiscale ion jet signatures with predicted reconnection site locations at the magnetopause

S. M. Petrinec[1], J. L. Burch[2], S. A. Fuselier[2,3], R. G. Gomez[2], W. Lewis[2], K. J. Trattner[4], R. Ergun[4], B. Mauk[5], C. J. Pollock[6], C. Schiff[6], R. J. Strangeway[7], C. T. Russell[7], T.-D. Phan[8], and D. Young[2]

[1]Lockheed Martin Advanced Technology Center, Palo Alto, California, USA, [2]Southwest Research Institute, San Antonio, Texas, USA, [3]Department of Physics and Astronomy, University of Texas at San Antonio, San Antonio, Texas, USA, [4]Laboratory for Atmospheric and Space Physics, University of Colorado Boulder, Boulder, Colorado, USA, [5]Johns Hopkins University Applied Physics Laboratory, Laurel, Maryland, USA, [6]NASA Goddard Space Flight Center, Greenbelt, Maryland, USA, [7]University of California, Los Angeles, California, USA, [8]Space Sciences Laboratory, University of California, Berkeley, California, USA

Key Points:
- Ion jets at the magnetopause compare favorably with a reconnection location model
- Plausible explanations are provided for the minority of jets that do not favorably compare with the model
- This model has been important for success of the MMS mission

Correspondence to:
S. M. Petrinec,
steven.m.petrinec@lmco.com

Citation:
Petrinec, S. M., et al. (2016), Comparison of Magnetospheric Multiscale ion jet signatures with predicted reconnection site locations at the magnetopause, *Geophys. Res. Lett.*, *43*, 5997–6004, doi:10.1002/2016GL069626.

Received 17 MAY 2016
Accepted 6 JUN 2016
Accepted article online 7 JUN 2016
Published online 22 JUN 2016

Abstract Magnetic reconnection at the Earth's magnetopause is the primary process by which solar wind plasma and energy gains access to the magnetosphere. One indication that magnetic reconnection is occurring is the observation of accelerated plasma as a jet tangential to the magnetopause. The direction of ion jets along the magnetopause surface as observed by the Fast Plasma Instrument (FPI) and the Hot Plasma Composition Analyzer (HPCA) instrument on board the recently launched Magnetospheric Multiscale (MMS) set of spacecraft is examined. For those cases where ion jets are clearly discerned, the direction of origin compares well statistically with the predicted location of magnetic reconnection using convected solar wind observations in conjunction with the Maximum Magnetic Shear model.

1. Introduction

The occurrence of steady collisionless magnetic reconnection at the magnetopause has long been established from indirect spacecraft observations [e.g., *Aubry et al.*, 1970; *Paschmann et al.*, 1979; *Sonnerup et al.*, 1981; *Gosling et al.*, 1986; *Phan et al.*, 2000], with support from numerous theoretical studies and numerical model results. However, the location where reconnection is most likely to occur at the magnetopause has been much less certain. When the interplanetary magnetic field (IMF) is strongly northward (with a small clock angle ($\tan^{-1}(B_y/B_z)$ near zero)), reconnection occurs tailward of the cusps [e.g., *Gosling et al.*, 1991; *Kessel et al.*, 1996; *Phan et al.*, 2003; *Fuselier et al.*, 2014a]. When there is a large *y* component to the IMF (in the geocentric solar magnetospheric coordinate system), reconnection occurs at the high-latitude flanks (sometimes referred to as a "sash") [e.g., *White et al.*, 1998]. When the IMF is southward, steady reconnection occurs at the dayside magnetopause sunward of the cusps. However, the dayside magnetopause region is large, spanning a surface area of several hundred square Earth radii (R_E), and reconnection can potentially occur over much of this region [e.g., *Cowley and Owen*, 1989]. In order to sample the site of magnetic reconnection directly, greater knowledge of the location of steady reconnection is required.

Different ideas to describe the most likely location of steady reconnection at the dayside magnetopause under southward IMF conditions have been put forth over the years. One idea was that reconnection would occur where the magnetic field on the two sides of the magnetopause is antiparallel. Some early works that examined where reconnection would occur along the magnetopause for this scenario include *Crooker* [1979] and *Luhmann et al.* [1984]. Here the loci of reconnection sites would lie along two discontinuous legs, located at lower latitudes along the magnetopause flanks and reaching the cusps near local noon. Another idea was that reconnection would most likely occur where the magnetosheath flow first contacts the magnetosphere (i.e., the standoff location) and would extend along the surface of the magnetopause as a continuous line away from this location. In this scenario, the reconnection line location and orientation is defined according to the criteria that there exists a component of the two fields on opposing sides of the magnetopause current layer which is antiparallel. This component reconnection model includes a nonzero guide field along the reconnection line. Some studies describing this scenario include *Sonnerup* [1974], *Gonzalez and Mozer* [1974], *Cowley* [1976], and *Moore et al.* [2002]. Other models of component reconnection location at the magnetopause did not impose this constraint [e.g., *Cowley and Owen*, 1989; *Swisdak and Drake*, 2007].

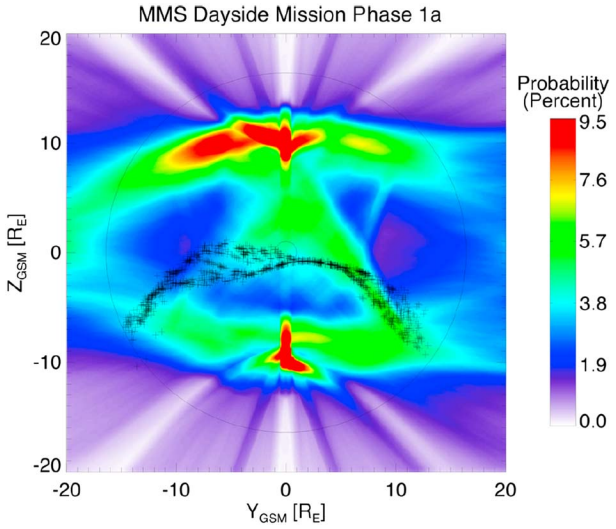

Figure 1. Probability map of reconnection line locations over the magnetopause surface (as viewed from the Sun), used to aid in the planning of the MMS ephemeris for targeting the magnetic reconnection sites (from *Fuselier et al.* [2014b]).

Berchem et al. [2003] and *Park et al.* [2006] examined reconnection locations with numerical models, considering where current densities or electric fields at the magnetopause are greatest. In the study of *Park et al.* [2006], this resulted in reconnection sites that could move in the north/south direction off the magnetopause standoff location as a function of the Earth's dipole tilt angle for strong IMF B_y.

A recent model developed from a detailed examination of many particle distribution velocity cutoffs in the cusps with consideration of time-of-flight and magnetic field mapping combines several of the features of the above-described scenarios and has come to be known as the Maximum Magnetic Shear model [e.g., *Trattner et al.*, 2007a]. The model predicts that for southward IMF but with a dominant IMF B_y, magnetic reconnection will occur along an extended line along the dayside magnetopause. However, instead of passing through the standoff location, the line proceeds along a ridge of maximum magnetic shear. When a strong IMF B_z ($155° < \tan^{-1}(B_y/B_z) < 205°$) or IMF B_x ($|B_{x\text{-GSM}}|/B_{\text{Tot}} > 0.7$) component is present, the reconnection location occurs along two separate legs which trace to high latitudes, as described by the antiparallel reconnection scenario [cf. *Fuselier et al.*, 2011; *Trattner et al.*, 2007a, 2007b, 2012].

The experience gained and lessons learned from previous missions, advanced numerical modeling, and theoretical models have been used to guide the Magnetospheric Multiscale (MMS) mission design [*Moore et al.*, 2013; *Burch et al.*, 2014]. The Maximum Magnetic Shear model had been favorably tested with previous spacecraft observations of ion jets and flow reversals [e.g., *Fuselier et al.*, 2011; *Dunlop et al.*, 2011; *Trattner et al.*, 2012] and there was enough confidence in its performance that it was used for ascertaining the location of magnetic reconnection. The model was used to produce probability maps of the magnetopause, utilizing solar wind magnetic field observations by the Advanced Composition Explorer (ACE) spacecraft from one solar cycle back. The predicted MMS magnetopause crossings were overlaid on this probability map, and the MMS orbital elements were optimized to try to target the highest probabilities (Figure 1) (from *Fuselier et al.* [2014b]) while maintaining a tight configuration and meeting requirements for several other mission operation parameters. Despite the challenge of targeting the spatially limited reconnection diffusion regions of the magnetopause far from the Earth (at altitudes of ~10–15 R_E), the success of this methodology has recently been demonstrated [*Burch et al.*, 2016]. In the remainder of this letter, we use MMS observations of ion jet signatures indicative of the occurrence of magnetopause reconnection to compare with the Maximum Magnetic Shear model estimate of the location of magnetic reconnection. It is noted that this particular survey is essentially a "single-spacecraft" study; that the full capabilities of the MMS mission (i.e., high-resolution multipoint observations with small spacecraft separations) are not exploited in this work.

2. Instrumentation and Data Sets

Multiple instruments on board the MMS spacecraft sample the plasma environment at high temporal, energy, and angular resolutions. One instrument is the Hot Plasma Composition Analyzer (HPCA) [*Young et al.*, 2014], which provides accurate measurements of major ion species (H^+, He^{++}, He^+, and O^+) in the energy range from 1 eV to 40 keV/e. Because the proton flux is the most populous species and can contaminate the fluxes of minor ions, the HPCA instrument employs a RF unit in the ion optics. This unit is prior to and independent of the time-of-flight section and reduces the proton flux relative to other species. Plasma

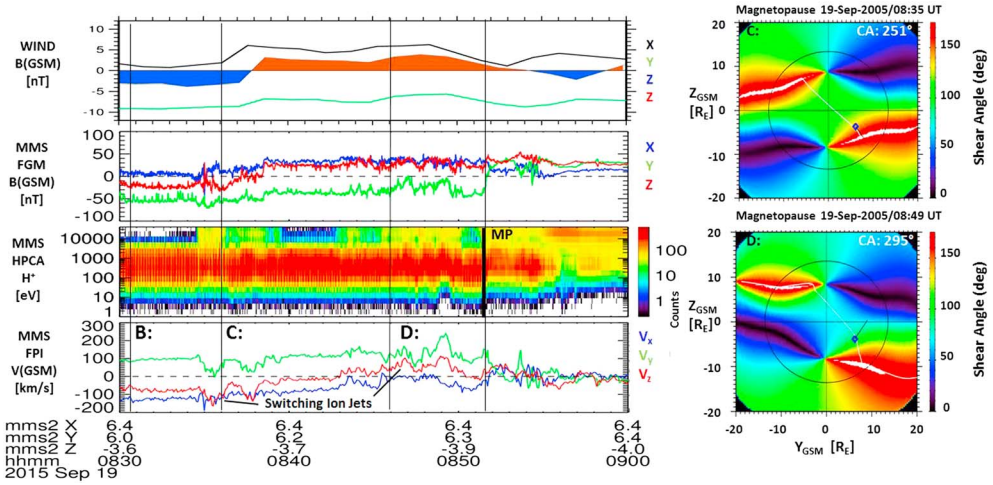

Figure 2. (left column) An example of in situ FGM, HPCA, and FPI observations of an ion jet reversal close to a magnetopause current sheet crossing. (right column) The model reconnection line for given IMF clock angle (CA) is in close proximity to the MMS spacecraft during these times (adapted from Figure 3 of *Trattner et al.*, this issue).

parameters are provided at half-spin (~10 s) temporal resolution. Further details are provided in *Burch et al.* [2005] and *Young et al.* [2014]. The HPCA observations are used in the description of the ion jet reversal example in section 3.

Plasma moments without mass discrimination are provided at even higher cadence by the Fast Plasma Instrument (FPI) on MMS [*Pollock et al.*, 2016]. The FPI ion moments (especially the velocity moment) are used to identify ion jets, as well as to determine the direction of flow. Magnetic field measurements are provided by the MMS Fluxgate Magnetometer (FGM) [*Russell et al.*, 2014; *Torbert et al.*, 2014]. The FGM observations are used to identify the magnetopause current layer in the ion jet reversal example and have been used by the MMS "Scientist in the Loop" (SITL) to identify the magnetopause and other intervals of interest. Solar wind measurements from the Wind mission [*Ogilvie et al.*, 1995; *Lepping et al.*, 1995] are convected to the Earth and are used to determine the reconnection line location along the dayside magnetopause.

3. Case of Observed Ion Jet Reversal

There are two methods by which the performance of the model in predicting the location of the reconnection line can be judged using in situ MMS observations. The first method is to identify intervals where a clear reversal of ion jets tangential to the magnetopause is observed. Such intervals have rarely been seen in past missions [e.g., *Trenchi et al.*, 2008; *Trattner et al.*, 2012], and so significant effort has gone into the MMS mission planning to target the reconnection site around which such flow reversals should be observed. One such identified interval of sudden flow reversal is presented in Figure 2. Figure 2 (left, second panel) shows the magnetic field of MMS1. A proton energy spectrogram from the HPCA instrument from the same spacecraft is shown in Figure 2 (left, third panel), while the velocity moment components determined from the FPI observations are displayed in Figure 2 (left, fourth panel). This interval spans the time 08:35–08:55 UT on 19 September 2015. At 08:35:00–08:36:30 UT and again at 08:37:10–08:38:30 UT two brief ion jets are observed along the $-Z_{GSM}$ direction. Associated with these jets are enhancements in ~10 keV protons, mixing magnetosheath, and magnetospheric protons. Several minutes later, ion jets are again observed but are in the opposite direction (enhancements along $+Z_{GSM}$). This behavior is consistent with a magnetopause reconnection line just northward of (above) the MMS spacecraft and then changing location so as to be just southward of (below) the MMS spacecraft. Maps of the magnetic shear angle across the magnetopause along with the MMS position and the location of the reconnection line are consistent with a close encounter with the reconnection line; lending support to the ability of the model to locate where magnetic reconnection is likely to occur at the dayside magnetopause. For this event, the northward motion of the reconnection line as determined from the order in which the jets are observed is in agreement with the motion of the reconnection line expected from the diamagnetic drift effect, given the negative B_y component as measured in the

magnetosheath [*Trenchi et al.*, 2015]. A more comprehensive discussion of this event is presented in *Trattner et al.* [2016].

As mentioned above, direct encounters with the reconnection line are rare. Far more common are observations of ion jets tangential to the magnetopause in one direction only [e.g., *Scurry et al.*, 1994]. A statistical analysis of a substantial number of such observations, while not precisely pinpointing the location of magnetic reconnection, can provide some constraints on the capabilities of the model. These cases can be indirectly compared with models such as the maximum magnetic shear reconnection line model, by calculating the percentage of events for which the observed jet directions are consistent with that expected from the location of the reconnection line relative to the observing spacecraft location.

4. Statistical Analysis of Observed Ion Jets

A listing of MMS complete magnetopause crossings has been compiled during Phase 1a of the MMS mission. As of mid-January 2016, there have been ~3200 magnetopause encounters by the MMS spacecraft. Many of these encounters were "partial" crossings, i.e., sampling of at least one boundary layers and/or crossing of the current layer at the magnetopause (but not a complete crossing between the magnetosphere proper and magnetosheath proper). For the purposes of this study, this large data set has been culled to only those for which complete magnetopause crossings (~1200) were identified by the MMS SITL. This set was then further reduced by considering only those crossings for which solar wind observations from the Wind spacecraft were available. In addition, only those events for which the convected Wind IMF clock angle was between 90° and 155°, or between 205° and 270°, and for which $|B_{x\text{-GSM}}|/B_{\text{Tot}} < 0.7$ are retained. These IMF constraints correspond to the ranges for which component reconnection along a contiguous reconnection line is present across the dayside magnetopause as postulated by the Maximum Magnetic Shear model. From this subset, only those crossings for which MMS was within 5 R_E (in the *YZ* projection plane) from the model Maximum Magnetic Shear model reconnection line (as determined using convected solar wind parameters with an average aberration angle of ~4°) are compared. In addition, some of the crossings in this reduced set could not be associated with clear ion jets that could be discerned from the FPI plasma moments due to boundary motions in association with variations in the solar wind speed and so were not included. Finally, although some ion jets were observed just outside the SITL selection intervals, they were not included in this initial survey because the IMF may have changed between the jet observation and the SITL interval. After consideration of all of the above constraints, 102 events associated with clear ion jets tangent to the magnetopause were identified for use in this survey. Relaxation of some of these strict criteria could dramatically increase the number of events for comparison, and a more extensive study will be undertaken in the future when MMS completes phase 1a, its first pass through the dayside magnetopause.

The cartoon depicted in Figure 3a illustrates sample MMS locations "north" and "south" of a model reconnection line. The view is from the Sun looking toward Earth. Black dashed arrows denote the normal direction from the reconnection line where it is closest to MMS, and the color of the arrow emanating from the MMS location indicates whether the ion jet is away (red) or toward (blue) the model reconnection line, by considering the angle (θ) between the normal to the reconnection line (along the shortest distance) and the vector describing the ion jet direction.

Figure 3b shows a mapping of the locations of MMS during the times of observation of the ion jets for the 102 identified events. At each location, the direction of the ion jet at the moment of maximum speed is shown. The great majority of observed ion jets are directed away from the model line (84/102), indicating a favorable comparison between model and observation. However, there are a few events for which the jet is directed toward the model reconnection line ($\theta > 90°$). It is noted that Figure 3b also implicitly shows that there is an orbital/event selection bias present. For intervals when MMS encounters the magnetopause far south of the equatorial plane and in the postnoon sector, the only way that the spacecraft can be within 5 R_E of the model reconnection line is if the IMF has negative $B_{y\text{-GSM}}$ and $B_{z\text{-GSM}}$ components (i.e., a clock angle between 205° and 270°). For the prenoon sector the IMF should have a positive $B_{y\text{-GSM}}$ and a negative $B_{z\text{-GSM}}$ (i.e., a clock angle between 90° and 155°).

A histogram of ion jet directions with respect to distance from the model reconnection line is shown in Figure 3c. Here the events are separated depending upon whether they were observed north or south of

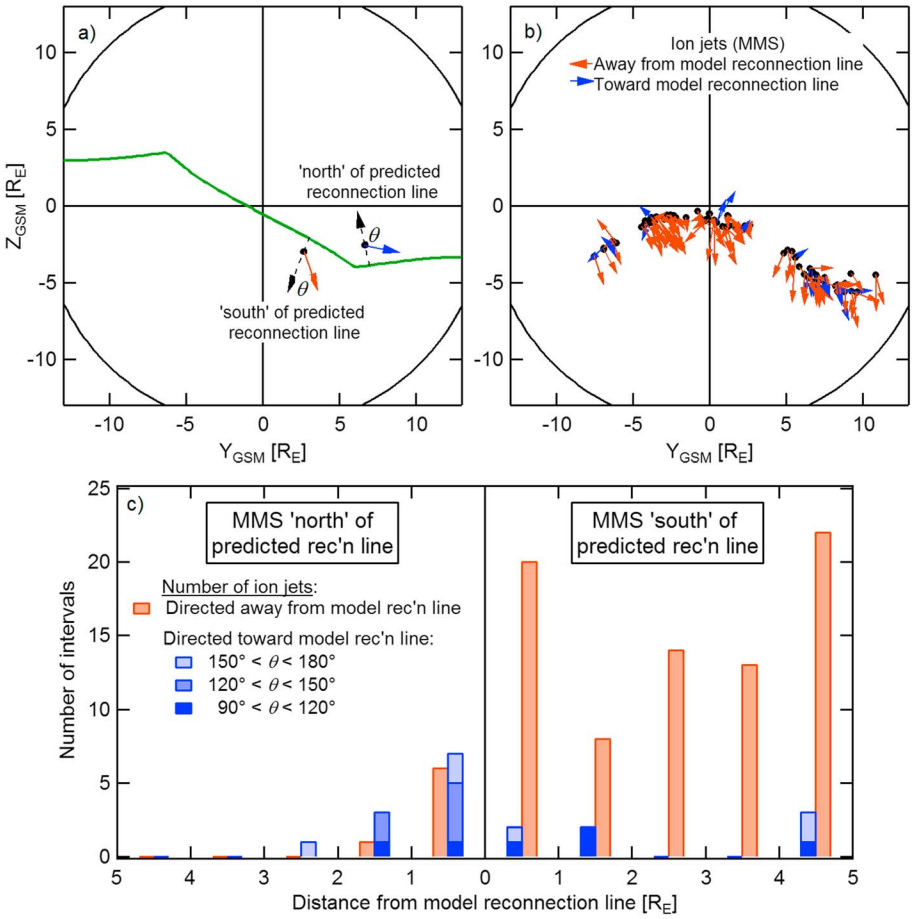

Figure 3. (a) A schematic contiguous reconnection line along the dayside magnetopause (green line) as viewed from the Sun. Black dashed arrows represent the normal to the line at the point closest to MMS. Solid arrows represent the direction of observed ion jets at the magnetopause. Red represents jets moving away from the model reconnection line ($\theta < 90°$); blue is toward the reconnection line ($\theta > 90°$). (b) Observed ion jets from 102 separate time intervals, as observed by FPI on board MMS. (c) Histogram of ion jet intervals, when MMS is north and south of the model reconnection line, respectively. Red bars signify those intervals where the jet is directed away from the model reconnection line; blue is toward the model reconnection line. The darkest blue segments are the number of intervals for which $90° < \theta < 120°$; the middle blue segments correspond to $120° < \theta < 150°$; the lightest blue segments correspond to $150° < \theta < 180°$.

the model reconnection line and are categorized according to whether the flow is directed away from or toward the model reconnection line (again, as red and blue bars, respectively). As can be seen, most of the events were observed when MMS was situated south of the model reconnection line. It can also be seen that many of the events that are directed toward the reconnection line actually occur close to (i.e., within 1 R_E of) the model reconnection line. The model line location is associated with an uncertainty of ~1 R_E [e.g., *Trattner et al.*, 2007*a*]; so several of the unfavorable comparisons can potentially be attributed to the inherent uncertainty of the model.

It is also noted that several of the jets which are directed toward the model reconnection line are also actually associated with an angle (θ) close to 90° and are closest to the antiparallel leg of the reconnection line along the flank. For these cases, however, the origin of the ion jet is likely not from the antiparallel leg but is much more likely to have originated further sunward along the magnetopause, from the contiguous component-merging line. In the histogram of Figure 3c, the blue bars are segmented with different shadings. The darkest blue segment corresponds to the number of intervals with calculated angles in the range $90° < \theta < 120°$; the middle blue segments correspond to $120° < \theta < 150°$; the light blue segments correspond to $150° < \theta < 180°$. Thus, of the 18 intervals that compare unfavorably with the Maximum Magnetic Shear model reconnection line, only five of these are greater than 1 R_E from the model line and are of large angle (i.e., $\theta > 120°$; directed

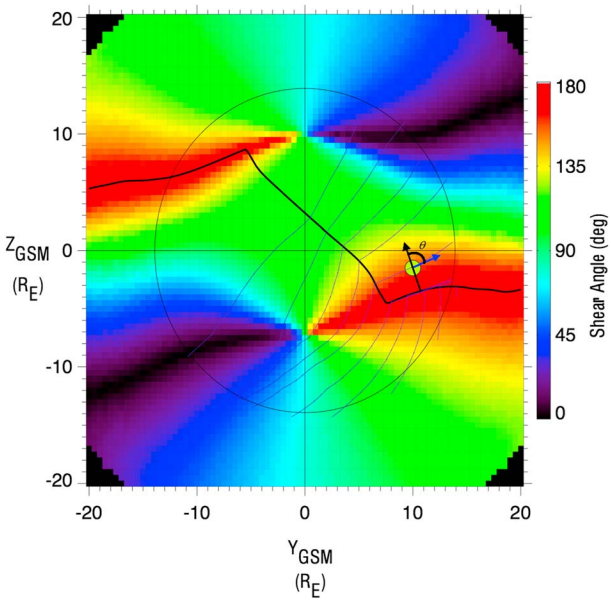

Figure 4. A schematic of the magnetic shear angle across the magnetopause (color shading), as viewed from the Sun. The black solid line represents the model reconnection line, and the small circle represents a sampling spacecraft (e.g., MMS). Thin blue lines represent flux tube motion away from the reconnection line. It can be seen that the closest distance between the spacecraft and the reconnection site (which in this case would be along the antiparallel leg) may not necessarily be the point of origin of the observed ion jet.

back toward the model reconnection line). Two of these five ion jet intervals (15 December 2015, at 10:57:54 and 10:58:34 UT) are actually the same jet observed twice as the magnetopause moves back and forth past the spacecraft within a single SITL selection interval.

Figure 4 shows an example for which the spacecraft location (small-filled circle) is closest to the dusk flank antiparallel leg. The motion of flux tubes accelerating from the reconnection line in the afternoon sector is mapped out as thin blue lines. The mapping has been performed in this example using the relations described by *Cowley and Owen* [1989] and used in a manner similar to that by *Cooling et al.* [2001] (i.e., $\boldsymbol{V}_{gm} = \boldsymbol{V}_{sh} \pm V_A(\mathbf{b}_{gm} - \mathbf{b}_{sh})$, where $\boldsymbol{V}_{gm}$: flux tube velocity; $\boldsymbol{V}_{sh}$: local magnetosheath velocity; V_A: local Alfvén speed; and $\mathbf{b}_{gm}$ and $\mathbf{b}_{sh}$ are the magnetic field unit vectors in the magnetosphere and magnetosheath, respectively). The calculated inner magnetosheath plasma parameters are determined from *Petrinec and Russell* [1997] for the magnetopause shape provided by the Tsyganenko magnetospheric field model [*Tsyganenko*, 1995]. It is seen that the flux tube trajectory that intersects the "spacecraft" does not originate from the antiparallel leg but from a location closer to local noon along the component-merging line. It is also closely aligned with the antiparallel leg so that the jet direction would be close to 90° from the direction normal to the antiparallel leg. Thus, some of the unfavorable comparisons in this statistical study are likely the result of the a priori assumption that the ion jet originates from the location along the model reconnection line that is physically closest to the spacecraft.

Finally, it has been assumed throughout this analysis that the reconnection site from which the ion jet has been observed is steady and stationary. These are strong assumptions, especially on the flanks where the local magnetosheath Alfvén Mach number can greatly exceed unity. Both the stationarity and persistence of the reconnection line location are important considerations that influence the ability to predict where reconnection may occur on the magnetopause. This topic remains an active field of research [e.g., *Petrinec et al.*, 2003; *Retinò et al.*, 2005; *Trenchi et al.*, 2008, 2015; *Dunlop et al.*, 2011; *Vines et al.*, 2015].

5. Summary

The Maximum Magnetic Shear model was used during the MMS mission design to maximize the probability of encountering magnetic reconnection at the magnetopause. The observance of ion jet reversals (e.g., Figure 1) and the direct sampling of diffusion regions [e.g., *Burch et al.*, 2016] demonstrate the success of this methodology. In this initial survey of MMS observations of ion jet directions at the magnetopause and comparison with the Maximum Magnetic Shear reconnection line (which depends upon solar wind conditions and Earth dipole tilt angle), it is found that a great majority of the MMS ion jet observations compare favorably with the model reconnection line prediction. It is also found that for several of the intervals for which the comparison is not favorable, plausible explanations can be found for most of these cases (e.g., inherent uncertainty of the model or misunderstanding of the point of origin of the ion jets). While this work does not completely validate the Maximum Magnetic Shear model, this initial survey of ion jets at the magnetopause suggests that the model does a reasonable job at predicting the relative location of reconnection sites as compared to the location of MMS.

Acknowledgments

The MMS mission is a culmination of years of effort from a large number of men and women. Collectively, they share in the scientific successes of the mission. All data are available to the general public through the MMS website. Research at Lockheed Martin is supported by NASA contract 499935Q. Research at LASP is also supported by NASA grant NNX11AJ09G and NNX14AF71G and NSF grant 1102572. The ISTP KP database (http://cdaweb.gsfc.nasa.gov/istp_public/) is also acknowledged.

References

Aubry, M. P., C. T. Russell, and M. G. Kivelson (1970), Inward motion of the magnetopause before a substorm, *J. Geophys. Res.*, *75*, 7018–7031, doi:10.1029/JA075i034p07018.

Berchem, J., S. A. Fuselier, S. Petrinec, H. U. Frey, and J. L. Burch (2003), Dayside proton aurora: Comparisons between global MHD simulations and IMAGE observations, *Space Sci. Rev.*, *109*, 313–349.

Burch, J. L., G. P. Miller, A. De Los Santos, C. J. Pollock, S. E. Pope, P. W. Valek, and D. T. Young (2005), Technique for increasing the dynamic range of space-borne ion composition instruments, *Rev. Sci. Instrum.*, *76*, 103301.

Burch, J. L., et al. (2014), Magnetospheric Multiscale overview and science objectives, *Space Sci. Rev.*, doi:10.1007/s11214-015-0164-9.

Burch, J. L., et al. (2016), Electron-scale measurements of magnetic reconnection in space, *Science*, doi:10.1126/science.aaf2939.

Cooling, B. M. A., C. J. Owen, and S. J. Schwartz (2001), Role of the magnetosheath flow in determining the motion of open flux tubes, *J. Geophys. Res.*, *106*, 18,763–18,775, doi:10.1029/2000JA000455.

Cowley, S. W. H. (1976), Comments on the merging of non-antiparallel magnetic fields, *J. Geophys. Res.*, *81*(19), 3455, doi:10.1029/JA081i019p03455.

Cowley, S. W. H., and C. J. Owen (1989), A simple illustrative model of open flux tube motion over the dayside magnetopause, *Planet. Space Sci.*, *37*, 1461–1475.

Crooker, N. U. (1979), Dayside merging and cusp geometry, *J. Geophys. Res.*, *84*, 951–959, doi:10.1029/JA084iA03p00951.

Dunlop, M. W., et al. (2011), Magnetopause reconnection across wide local time, *Ann. Geophys.*, *29*, 1683–1697.

Fuselier, S. A., K. J. Trattner, and S. M. Petrinec (2011), Antiparallel and component reconnection at the dayside magnetopause, *J. Geophys. Res.*, *116*, A10227, doi:10.1029/2011JA016888.

Fuselier, S. A., S. M. Petrinec, K. J. Trattner, and B. Lavraud (2014a), Magnetic field topology for northward IMF reconnection: Ion observations, *J. Geophys. Res. Space Physics*, *119*, 9051–9071, doi:10.1002/2014JA020351.

Fuselier, S. A., W. S. Lewis, C. Schiff, R. Ergun, J. L. Burch, S. M. Petrinec, and K. J. Trattner (2014b), Magnetospheric Multiscale science mission profile and operations, *Space Sci. Rev.*, doi:10.1007/s11214-014-0087-x.

Gonzalez, W. D., and F. S. Mozer (1974), A quantitative model for the potential resulting from reconnection with an arbitrary interplanetary magnetic field, *J. Geophys. Res.*, *79*, 4186–4194, doi:10.1029/JA079i028p04186.

Gosling, J. T., M. F. Thomsen, S. J. Bame, and C. T. Russell (1986), Accelerated plasma flows at the near-tail magnetopause, *J. Geophys. Res.*, *91*, 3029–3041, doi:10.1029/JA091iA03p03029.

Gosling, J. T., M. F. Thomsen, S. J. Bame, R. C. Elphic, and C. T. Russell (1991), Observations of reconnection of interplanetary and lobe magnetic field lines at the high-latitude magnetopause, *J. Geophys. Res.*, *96*, 14,097–14,106, doi:10.1029/91JA01139.

Kessel, R. L., S.-H. Chen, J. L. Green, S. F. Fung, S. A. Boardsen, L. C. Tan, T. E. Eastman, J. D. Craven, and L. A. Frank (1996), Evidence of high-latitude reconnecting during northward IMF: Hawkeye observations, *Geophys. Res. Lett.*, *23*, 583–586, doi:10.1029/95GL03083.

Lepping, R. P., et al. (1995), The Wind magnetic field instrument, in *The Global Geospace Mission*, edited by C. T. Russell, pp. 207–227, Kluwer Academic Press, Norwell, Mass.

Luhmann, J. R., R. J. Walker, C. T. Russell, N. U. Crooker, J. R. Spreiter, and S. S. Stahara (1984), Patterns of potential magnetic field merging sites on the dayside magnetopause, *J. Geophys. Res.*, *89*, 1739–1742, doi:10.1029/JA089iA03p01739.

Moore, T. E., M.-C. Fok, and M. O. Chandler (2002), The dayside reconnection X line, *J. Geophys. Res.*, *107*(A10), 1332, doi:10.1029/2002JA009381.

Moore, T. E., J. L. Burch, W. S. Daughton, S. A. Fuselier, H. Hasegawa, S. M. Petrinec, and Z. Pu (2013), Multiscale studies of the three-dimensional dayside X-line, *J. Atmos. Sol. Terr. Phys.*, *99*, 32–40.

Ogilvie, K. W., et al. (1995), SWE: A comprehensive plasma instrument for the Wind spacecraft, in *The Global Geospace Mission*, edited by C. T. Russell, pp. 55–77, Kluwer Acad. Press, Norwell, Mass.

Park, K. S., T. Ogino, and R. J. Walker (2006), On the importance of antiparallel reconnection when the dipole tilt and IMF B_y are nonzero, *J. Geophys. Res.*, *111*, A05202, doi:10.1029/2004JA010972.

Paschmann, G., N. Sckopke, S. J. Bame, J. R. Asbridge, J. T. Gosling, C. T. Russell, and E. W. Greenstadt (1979), Plasma acceleration at the Earth's magnetopause: Evidence for reconnection, *Nature*, *282*, 243–246.

Petrinec, S. M., and C. T. Russell (1997), Hydrodynamic and MHD equations across the bow shock and along the surfaces of planetary obstacles, *Space Sci. Rev.*, *79*(3/4), 757–791.

Petrinec, S. M., K. J. Trattner, and S. A. Fuselier (2003), Steady reconnection during intervals of northward IMF: Implications for magnetosheath properties, *J. Geophys. Res.*, *108*(A12), 1458, doi:10.1029/2003JA009979.

Phan, T. D., et al. (2000), Extended magnetic reconnection at the Earth's magnetopause from detection of bi-directional jets, *Nature*, *404*, 848–850.

Phan, T. D., et al. (2003), Simultaneous Cluster and IMAGE observations of cusp reconnection and auroral proton spot for northward IMF, *Geophys. Res. Lett.*, *30*(10), 1509, doi:10.1029/2003GL016885.

Pollock, C., et al. (2016), Fast plasma investigation for Magnetospheric Multiscale, *Space Sci. Rev.*, *199*, 331–406, doi:10.1007/s11214-016-0245-4.

Retinò, A., et al. (2005), Cluster multispacecraft observations at the high-latitude duskside magnetopause: Implications for continuous and component magnetic reconnection, *Ann. Geophys.*, *23*, 461–473, doi:10.5194/angeo-23-461-2005.

Russell, C. T., et al. (2014), The Magnetospheric Multiscale magnetometers, *Space Sci. Rev.*, doi:10.1007/s11214-014-0057-3.

Scurry, L., C. T. Russell, and J. T. Gosling (1994), A statistical study of accelerated flow events at the dayside magnetopause, *J. Geophys. Res.*, *99*(A8), 14,815–14,829, doi:10.1029/94JA00793.

Sonnerup, B. U. Ö. (1974), The reconnecting magnetosphere, in *Magnetospheric Physics, Proceedings of the Advanced Summer Institute, held at Sheffield, UK, 1973, Dortrecht: Reidel, Astrophysics and Space Science Library*, vol. 44, edited by B. M. McCormas, pp. 23.

Sonnerup, B. U. Ö., G. Paschmann, I. Papamastorakis, N. Sckopke, G. Haerendel, S. J. Bame, J. R. Asbridge, J. T. Gosling, and C. T. Russell (1981), Evidence for magnetic field reconnection at the Earth's magnetopause, *J. Geophys. Res.*, *86*, 10,049–10,067, doi:10.1029/JA086iA12p10049.

Swisdak, M., and J. F. Drake (2007), Orientation of the reconnection X-line, *Geophys. Res. Lett.*, *34*, L11106, doi:10.1029/2007GL029815.

Torbert, R. B., et al. (2014), The FIELDS instrument suite on MMS: Scientific objectives, measurements, and data products, *Space Sci. Rev.*, doi:10.1007/s11214-014-0109-8.

Trattner, K. J., J. S. Mulcock, S. M. Petrinec, and S. A. Fuselier (2007a), Location of the reconnection line at the magnetopause during southward IMF conditions, *Geophys. Res. Lett.*, *34*, L03108, doi:10.1029/2006GL028397.

Trattner, K. J., J. S. Mulcock, S. M. Petrinec, and S. A. Fuselier (2007b), Probing the boundary between antiparallel and component reconnection during southward interplanetary magnetic field conditions, *J. Geophys. Res.*, *112*, A08210, doi:10.1029/2007JA012270.

Trattner, K. J., S. M. Petrinec, S. A. Fuselier, and T. D. Phan (2012), The location of reconnection at the magnetopause: Testing the maximum magnetic shear model with THEMIS observations, *J. Geophys. Res.*, *117*, A01201, doi:10.1029/2011JA016959.

Trattner, K. J., et al. (2016), The response time of the magnetopause reconnection location to changes in the solar wind: MMS case study, *Geophys. Res. Lett.*, *45*, doi:10.1002/2016GL068554 (in press).

Trenchi, L., M. F. Marcucci, G. Pallocchia, G. Consolini, M. B. Bavassano Cattaneo, A. M. Di Lellis, H. Rème, L. Kistler, C. M. Carr, and J. B. Cao (2008), Occurrence of reconnection jets at the dayside magnetopause: Double Star observations, *J. Geophys. Res.*, *113*, A07S10, doi:10.1029/2007JA012774.

Trenchi, L., M. F. Marcucci, and R. C. Fear (2015), The effect of diamagnetic drift on motion of the dayside magnetopause reconnection line, *Geophys. Res. Lett.*, *42*, 6129–6136, doi:10.1002/2015GL065213.

Tsyganenko, N. (1995), Modeling the Earth's magnetospheric magnetic field confined within a realistic magnetopause, *J. Geophys. Res.*, *100*, 5599–5612, doi:10.1029/94JA03193.

Vines, S. K., S. A. Fuselier, K. J. Trattner, S. M. Petrinec, and J. F. Drake (2015), Ion acceleration dependence on magnetic shear angle in dayside magnetopause reconnection, *J. Geophys. Res. Space. Physics*, *120*, 7255–7269, doi:10.1002/2015JA021464.

White, W. W., G. L. Siscoe, G. M. Erickson, Z. Kaymaz, N. C. Maynard, K. D. Siebert, B. U. Ö. Sonnerup, and D. R. Weimer (1998), The magnetospheric sash and the cross-tail S, *Geophys. Res. Lett.*, *25*, 1605–1608, doi:10.1029/98GL50865.

Young, D. T., et al. (2014), Hot plasma composition analyzer for the Magnetospheric Multiscale mission, *Space Sci. Rev.*, doi:10.1007/s11214-014-0049-6.